

Ultralong fibre-optic distributed Raman temperature sensor

A.G. Kuznetsov, D.S. Kharenko, S.A. Babin, I.B. Tsydenzhapov, I.S. Shelemba

Abstract. We have demonstrated an ultralong (up to 85 km in length) all-fibre Raman temperature sensor which utilises SMF-28 standard single-mode telecom fibre and a 1.63- μm probe signal source. The probe signal from the laser diode is amplified by a Raman fibre amplifier. The temperature along a 85-km-long fibre line has been measured with an accuracy of 8 °C and spatial resolution of 800 m or better.

Keywords: distributed temperature sensor, Raman scattering, fibre-optic link.

1. Introduction

Fibre-optic sensing systems are the subject of intense research and are used in diverse applications: coal, petroleum and gas production; structural health monitoring; aircraft engineering; etc. Fibre-optic sensors allow one to measure many parameters of media: temperature, pressure, strain, magnetic field and others [1, 2]. An important point is that the sensing element of such devices can be located far away (up to several tens of kilometres from the control and interrogation unit), with no need to connect it to power supply lines, and only the optical signal propagating in a fibre-optic link is used for measurements. Even though this area of technology is relatively young, the fibre-optic sensor market is one of the most rapidly growing in the world, and in some fields such sensors have almost completely replaced their classic electrical analogues. The key advantages of the fibre-optic sensors are their small size, reliability, long-term operation stability, stability to electromagnetic interference and chemical inertness.

In this paper, we present a distributed temperature sensor that utilises Raman scattering in optical fibre. Analysis of the dynamics of the intensity of the Stokes and anti-Stokes Raman signals makes it possible to calculate the temperature profile along the entire fibre. As a rule, a laser diode or fibre laser emitting at a wavelength near 1.55 μm is used as a probe

pulse source for distributed Raman sensors. If necessary, its output is amplified by erbium fibre amplifiers to required peak powers [3]. The above wavelength is convenient for researchers because it lies within the transmission window of optical fibre and is a sort of standard for telecommunication systems. Optical components for this spectral range – both active (laser diodes, modulators, erbium fibre amplifiers and others) and passive (isolators, circulators, fibre couplers and others) – are commercially available and relatively cheap.

One factor limiting the performance of fibre-optic sensors is stimulated Raman scattering, which makes it impossible to raise the probe signal power and, hence, the power of useful scattered light to above a certain threshold. The vast majority of commercial distributed sensor systems utilise multimode fibre, which has a lower power density and, accordingly, a higher SRS threshold owing to the large diameter of its core [4]. This offers the possibility of substantially increasing the source power and improving the main parameters of the measuring system. At the same time, the use of multimode fibre has a number of drawbacks in comparison with single-mode fibre: it has substantially higher losses (~ 0.5 dB km^{-1} in multimode fibre against ~ 0.2 dB km^{-1} in single-mode fibre), which limits the maximum link length. In addition, modal dispersion increases the probe pulse duration and degrades the spatial resolution of the sensor. Because of this, the maximum length of multimode fibre-based temperature sensors usually does not exceed 8 km, with typical temperature and spatial resolutions of 1 °C and 2 m, respectively [5]. If single-mode fibre is used as a sensing element, the measuring fibre line can be as long as 16 km [6]. The existing sensor interrogation techniques (cyclic and simplex coding and others) allow the maximum fibre line length to be increased further, up to 55 km [7].

In this paper, we demonstrate the possibility of increasing the maximum length (to 85 km) of an all-fibre distributed temperature sensor by using probe light at wavelengths above 1.6 μm . The choice of such operating wavelengths is suggested by several factors, which prove to be critical for the ability to produce an ultralong temperature sensor. First, the relatively weak anti-Stokes Raman signal then lies in the 1.5- μm transmission window, where losses are lower than at 1.4 μm . Second, the Stokes signal will then lie around 1.7 μm , where losses are considerably higher and, hence, the SRS threshold is also higher, which offers the possibility of raising the probe light power and, therefore, the intensity of the anti-Stokes Raman signal.

2. Theory and measurement principle

Raman scattering is an inelastic process accompanied by a marked change in the frequency of the light being scattered: if a source emits monochromatic light, the scattered light spec-

A.G. Kuznetsov, D.S. Kharenko, S.A. Babin Institute of Automation and Electrometry, Siberian Branch, Russian Academy of Sciences, prosp. Akad. Koptyuga 1, 630090 Novosibirsk, Russia; Novosibirsk State University, ul. Pirogova 2, 630090 Novosibirsk, Russia; e-mail: leks.kuznecov@gmail.com;

I.B. Tsydenzhapov Novosibirsk State University, ul. Pirogova 2, 630090 Novosibirsk, Russia; Inversion-Sensor Ltd., ul. 25 Oktyabrya 106, 614990 Perm, Russia; e-mail: i.b.tsydenzhapov@i-sensor.ru;

I.S. Shelemba Inversion-Sensor Ltd., ul. 25 Oktyabrya 106, 614990 Perm, Russia; e-mail: shelemba@i-sensor.ru

Received 22 May 2017; revision received 26 July 2017
Kvantovaya Elektronika 47 (10) 967–970 (2017)
Translated by O.M. Tsarev

trum contains, in addition to elastic (Rayleigh) scattering at (unshifted) frequency ν_0 , lines whose number and position are closely related to the molecular structure of the substance. The transition of a molecule from the ground state to an excited one produces a Raman line at a lower frequency: $\nu_s = \nu_0 - \Delta\nu$ (Stokes signal). Similarly, the transition of a molecule from an excited state to the ground state increases the frequency of the scattered light by $\Delta\nu$: $\nu_a = \nu_0 + \Delta\nu$ (anti-Stokes signal).

In silica fibre, the Raman signals are separated from the centre frequency by approximately 440 cm^{-1} [8]. Excited state population depends on the temperature of the substance and, hence, the anti-Stokes intensity is also temperature-dependent. The power of the scattered light at time $t = 2Ln/c$ (where n is the refractive index and c is the speed of light) at point $z = L$ is represented by the following expressions for the Stokes, anti-Stokes and Rayleigh signals [9, 10]:

$$P_s(T) = P_0 K_s S v_s^4 \exp[-(\alpha_0 + \alpha_s)L] R_s(T) \tau_p, \quad (1)$$

$$P_a(T) = P_0 K_a S v_a^4 \exp[-(\alpha_0 + \alpha_a)L] R_a(T) \tau_p, \quad (2)$$

$$P_R(T) = P_0 K_R S v_R^4 \exp(-2\alpha_0 L) \tau_p, \quad (3)$$

where P_0 is the probe pulse power; K_a , K_s and K_R are the anti-Stokes, Stokes and Rayleigh scattering coefficients; S is the backscatter factor in the fibre; T is the absolute temperature; τ_p is the probe pulse duration; α_0 , α_a and α_s are the linear probe, anti-Stokes and Stokes signal losses; and $R_s(T)$ and $R_a(T)$ are temperature-dependent coefficients related to the populations of the lower and upper levels. The populations of the levels are described by the Boltzmann distribution:

$$R_s(T) = [1 - \exp(-h\Delta\nu/k_B T)]^{-1}, \quad (4)$$

$$R_a(T) = [\exp(h\Delta\nu/k_B T) - 1]^{-1}, \quad (5)$$

where k_B is the Boltzmann constant and h is the Planck constant.

Thus, measuring the anti-Stokes power P_a in the fibre and normalising it to the Stokes (P_s) or Rayleigh (P_R) scattering power in order to exclude non-temperature effects (such as bending or fusion splice losses), we can calculate the temperature using one of the following relations:

$$\frac{P_a(T)}{P_s(T)} \sim \left(\frac{v_a}{v_s}\right)^4 \exp\left(-\frac{h\Delta\nu}{k_B T}\right) \exp[-(\alpha_a - \alpha_s)L], \quad (6)$$

$$\frac{P_a(T)}{P_R} \sim \left(\frac{v_a}{v_R}\right)^4 \frac{\exp[-(\alpha_a - \alpha_0)L]}{\exp(h\Delta\nu/k_B T) - 1}. \quad (7)$$

In real temperature measurement experiments, the temperature cannot be accurately calculated by formulas (6) and (7) because of a variety of factors, such as different shapes of the spectral filter for different components and different spectral responses of photodiodes, and the instrument should be precalibrated [11]. For this purpose, a part of the fibre, so called dummy fibre, is placed in a thermostat at a known temperature T_0 , one measures $P_a(T_0)/P_s(T_0)$ [or $P_a(T_0)/P_R$], and the results are used to correct the constants in (6) and (7).

3. Experimental

As a probe source, we used a commercially available 1628-nm NEC laser diode with a maximum peak power of 125 mW. To amplify its output, we made a Raman amplifier based on a 10-km length of OFS NZ DSF dispersion-shifted fibre, which was pumped by a fibre laser at a wavelength of 1530 nm (Fig. 1). The pump laser had an erbium fibre ring cavity and its output was amplified by an Er–Yb fibre amplifier. The maximum output power at $\lambda_{\text{pump}} = 1530 \text{ nm}$ after the amplifier was 1.7 W. The laser diode signal at a wavelength of 1628 nm and pump light (1530 nm) were coupled into the Raman amplifier using a WDM coupler. At a pump power of

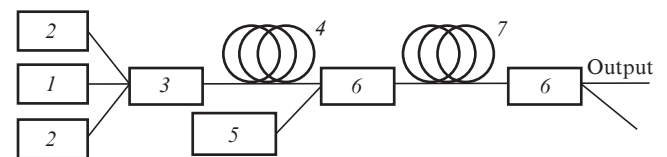


Figure 1. Schematic of the Raman amplification of a 1628-nm probe signal: (1) erbium fibre laser (1530 nm); (2) multimode pump laser diode (976 nm; power, 8 W); (3) pump combiner; (4) Er/Yb-codoped fibre; (5) pulsed laser diode (1628 nm); (6) WDM 1530/1630 nm; (7) Raman amplifier based on a 10-km length of NZ DSF single-mode fibre.

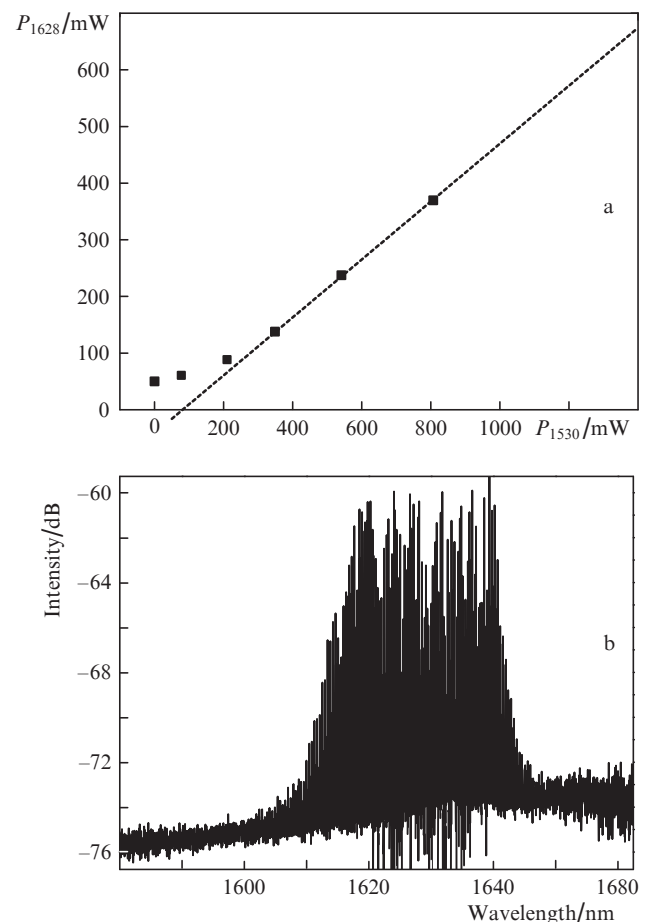


Figure 2. (a) Output power of the amplified signal (1628 nm) as a function of 1530-nm pump power and (b) the corresponding probe signal spectrum at the Raman amplifier output.

810 mW, the probe signal was amplified to a peak power of 370 mW. Further amplification was limited by the interpulse SRS threshold. Figure 2 shows the probe laser output spectrum and the signal power as a function of pump power.

Figure 3 shows a schematic of the Raman measurements. Laser pulses with a repetition rate of 100 Hz and duration $\tau_p = 8 \mu\text{s}$ are launched into a 85-km fibre line (Fujikura SMF-28) consisting of three fibre spools, 50, 30 and 5 km in length, spliced in series. The 5-km-long fibre spool, placed in a thermostat at the end of the line, is heated to about 60°C . Passing through a spectral filter, the Raman backscatter signal is divided into Rayleigh and anti-Stokes signals and directed to two photodiodes with a bandwidth of 10 MHz. The analogue signal from the photodiodes arrives at an ADC and then at a computer, where the signals are analysed and the temperature is calculated by formula (7).

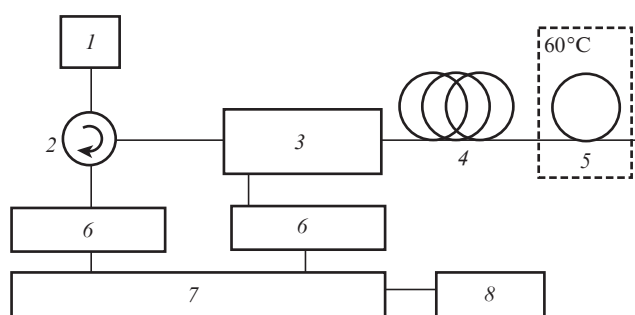


Figure 3. Schematic of the Raman measurements: (1) pulsed probe laser with a Raman amplifier (1628 nm); (2) circulator; (3) optical signal filtering system; (4) 80-km length of optical fibre at room temperature; (5) 5-km length of optical fibre in a thermostat; (6) photodiodes detecting the corresponding spectral scattering components; (7) ADC; (8) signal processing and temperature calculation unit (computer).

As a spectral filter, we used commercially available thin-film wavelength division multiplexers, FWDMs, for the L/C telecom range (their transmission spectrum is presented in Fig. 4). To maximise the signal filtering efficiency, three couplers were connected in series, so that the backscatter signal

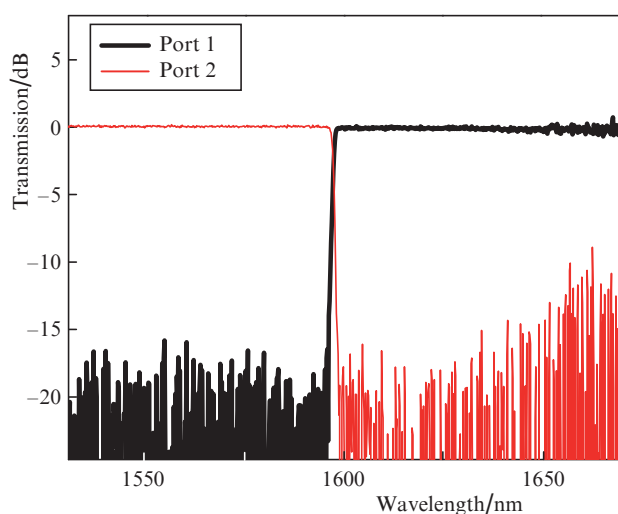


Figure 4. Transmission spectrum of the FWDMs.

was divided by the filter into two channels (1.5 and 1.6 μm) and detected by avalanche photodiodes.

4. Results and discussion

Figure 5a shows reflectograms of the Rayleigh and anti-Stokes Raman scattering intensity in the 85-km line after $60000\times$ averaging in order to minimise the noise. At the end of the anti-Stokes reflectogram, the intensity is observed to increase, which corresponds to heating of the fibre segment. Attention should also be paid to the fact that, in our case, the broad probe signal spectrum (Fig. 2b) allows reflectograms to be recorded with acceptable quality in lines up to 90 km in length, unlike in the case of a phase-sensitive Rayleigh reflectometer [12], where the effect of modulation instability [13] at peak powers above 1 W significantly reduces the operating length of the fibre line, making it less than 10 km.

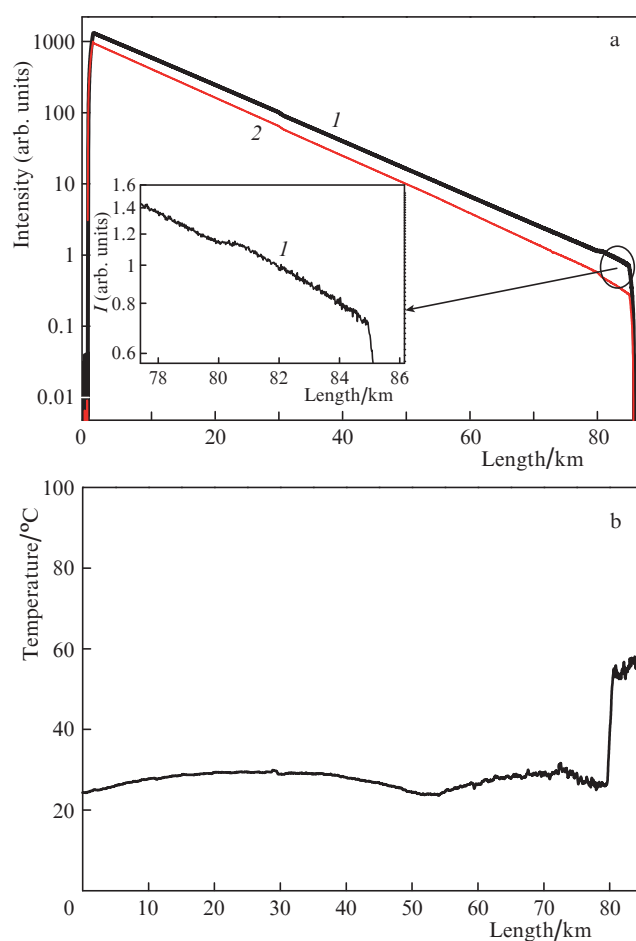


Figure 5. (a) Reflectograms of the (1) anti-Stokes and (2) Rayleigh scattering intensities and (b) calculated temperature profile along the fibre.

Using these data and formula (7), we calculated the temperature along the fibre line. The temperature profile is shown in Fig. 5b. The accuracy in our temperature measurements was 8°C , and the spatial resolution, determined by the pulse duration τ_p , was 800 m in our case ($\tau_p = 8 \mu\text{s}$). Note that, even though the 80-km-long fibre line is maintained at room temperature during the measurements, Fig. 5b demonstrates a distortion of the temperature profile, with a minimum around

50 km, i.e. at the fusion splice between the 50- and 30-km-long fibre spools, because different losses at wavelengths of 1.6 and 1.5 μm were observed at this point and because normalisation (7) does not completely exclude fusion splice losses. To more accurately measure the temperature in a fibre line containing one or a few fibre fusion splices, it is necessary either to take into account the difference in spectral losses at the splices or to probe the sensitive part of the fibre using two distinct sources: one at a wavelength of 1.5 μm , where Rayleigh scattering is detected, and the other at 1.6 μm , where the anti-Stokes Raman signal is detected (together with a wavelength near 1.5 μm),

5. Conclusions

This study has demonstrated the possibility of temperature measurements with a single-mode fibre Raman sensor up to 85 km in length. A distinctive feature of the sensor is its all-fibre scheme with a probe signal source at a wavelength of 1.63 μm . The transition to the 1.6- μm spectral range made it possible to reduce the anti-Stokes signal loss and increase the Stokes signal loss, which allowed the SRS threshold to be raised.

The maximum length of the measuring fibre line was 85 km, with a 800-m spatial resolution and 8°C accuracy in our temperature measurements. In future work, optimisation of the Raman amplifier and the use of, for example, simplex coding will allow both spatial and temperature resolution to be substantially improved. The described temperature measurement system can be used to monitor leaks in pipes and detect heating places in high-voltage transmission lines and other extended objects. In particular, a prototype of this device was tested in an ice melting facility in the case of ground wire freezing along high-voltage lines, where the spatial resolution obtained was sufficient for monitoring the temperature of extended parts with and without congelation.

Acknowledgements. We are grateful to I.Ya. Vevo for fabricating the fibre couplers. This work was supported by the Siberian Branch of the Russian Academy of Sciences (SB RAS) (integrated research project) and carried out using equipment at the Spectroscopy and Optics Shared Research Facilities Centre, Institute of Automation and Electrometry, SB RAS.

References

1. Kul'chin Yu.N. *Raspredelemnye volokonno-opticheskie izmeritel'nye sistemy* (Distributed Fibre-Optic Measuring Systems) (Moscow: Fizmatlit, 2004).
2. Yu F.T.S., Yin S. *Fiber Optic Sensors* (CRC Press, 2002).
3. Kuznetsov A.G., Babin S.A., Shelemba I.S. *Quantum Electron.*, **39** (11), 1078 (2009) [*Kvantovaya Elektron.*, **39** (11), 1078 (2009)].
4. Stierlin R., Ricka J., Zysset B., Bättig R., Weber Heinz P., Binkert T., Borer W.J. *Appl. Opt.*, **26** (8), 1368 (1987).
5. Bharath Kumar Lagishetty, Balaji Srinivasan, in *Proc. ICOP 2009* (Chandigarh, India, 2009).
6. Karamehmedovic E., Feuchter T., in *Proc. Photonics West* (San Jose, CA, USA, 2004).
7. Muanenda Y.S., Taki M., Nannipieri T., et al. *J. Lightwave Technol.*, **34** (2), 342 (2016).
8. Long D.A. *Raman Spectroscopy* (New York: McGraw-Hill, 1977).
9. Meng Ling, Jiang Ming-shun, Sui Qing-mei. *Optoelectron. Lett.*, **4** (6), 0415 (2008).
10. Farahani M.A., Gogolla T. *J. Lightwave Technol.*, **17** (8), 1379 (1999).
11. Stoddart P.R., Cadusch P.J., Pearce J.B., Vukovic D., Nagarajah C.R., Booth D.J. *Meas. Sci. Technol.*, **16**, 1299 (2005).
12. Tosoni O., Aksenov S.B., Podivilov E.V., Babin S.A. *Quantum Electron.*, **40** (10), 887 (2010) [*Kvantovaya Elektron.*, **40** (10), 887 (2010)].
13. Ismagulov A.E., Babin S.A., Podivilov E.V., Fedoruk M.P., Shelemba I.S., Shtyrina O.V. *Quantum Electron.*, **39** (8), 765 (2009) [*Kvantovaya Elektron.*, **39** (8), 765 (2009)].